Effects of Recovery Behavior and Strain-Rate Dependence of Stress–Strain Curve on Prediction Accuracy of Thermal Stress Analysis During Casting

YUICHI MOTOYAMA, HIDETOSHI SHIGA, TAKESHI SATO, HIROSHI KAMBE, and MAKOTO YOSHIDA

Recovery behavior (recovery) and strain-rate dependence of the stress–strain curve (strain-rate dependence) are incorporated into constitutive equations of alloys to predict residual stress and thermal stress during casting. Nevertheless, few studies have systematically investigated the effects of these metallurgical phenomena on the prediction accuracy of thermal stress in a casting. This study compares the thermal stress analysis results with *in situ* thermal stress measurement results of an Al-Si-Cu specimen during casting. The results underscore the importance for the alloy constitutive equation of incorporating strain-rate dependence to predict thermal stress that develops at high temperatures where the alloy shows strong strain-rate dependence of the stress–strain curve. However, the prediction accuracy of the thermal stress developed at low temperatures did not improve by considering the strain-rate dependence. Incorporating recovery into the constitutive equation improved the accuracy of the simulated thermal stress at low temperatures. Results of comparison implied that the constitutive equation should include strain-rate dependence to simulate defects that develop from thermal stress at high temperatures, such as hot tearing and hot cracking. Recovery should be incorporated into the alloy constitutive equation to predict the casting residual stress and deformation caused by the thermal stress developed mainly in the low temperature range.

DOI: 10.1007/s11661-017-4060-7

I. INTRODUCTION

RESIDUAL stress and deformation in castings are crucially important issues not only for producing components that have high-precision shapes but also for managing the fatigue life of casting components. Therefore, several researchers of casting processes have used thermal stress analysis *via* computer-aided engineering (CAE). The prediction accuracy of the thermal stress analysis is dependent mainly on the constitutive equation of cast alloys and the mechanical properties included in that equation. This study specifically addressed the thermal stress analysis of Al-Si-Cu casting. In this section, this study reviews previous alloy constitutive equations used for thermal stress analysis during casting. Additionally, we examine the mechanical properties used for thermal stress analysis of the Al-Si-Cu alloy during casting.

YUICHI MOTOYAMA is with the Advanced Manufacturing Research Institute, National Institute of Advanced Industrial Science and Technology, 1-2-1, Tsukuba, Ibaraki, 305-8564 Japan. Contact e-mail: y.motoyama@aist.go.jp HIDETOSHI SHIGA, TAKESHI SATO, and HIROSHI KAMBE are with the Nissan Motor Co. Ltd., 6-1, Daikokucho Tsurumi-ku, Yokohama-shi, Kanagawa 230-0053, Japan. MAKOTO YOSHIDA is with the Kagami Memorial Research Institute for Material Science and Technology, Waseda University, 2-8-26, Nishiwaseda, Shinjuku-ku, Tokyo, 69-0051, Japan.

Manuscript submitted December 1, 2016.
Article published online March 13, 2017

A. *Alloy Constitutive Equations Used for Thermal Stress Analysis During Casting*

Thermal stress develops in the casting because of differences in the cooling rate during cooling. Therefore, the constitutive equation of the casting should incorporate the following metallurgical phenomena. The strain-rate dependence of the stress–strain curve (hereinafter designated as the strain-rate dependence) at a high temperature is a well-known mechanical behavior in an alloy. At high strain-rates, the flow stress becomes higher. At lower temperatures, the alloy does not normally show low strain-rate sensitivity.[1,2] Recrystallization and recovery occur at high temperatures. Therefore, inelastic strain developing at high temperatures does not contribute to strain-hardening at low temperatures. With the decrease in temperature, the amount of inelastic strain that contributes to strain-hardening increases gradually. Finally, all amount of the inelastic strain causes strain-hardening at room temperature. The previous studies explained that the inelastic strain developed at high temperatures does not affect the strain-hardening behavior in low temperature range for the reason that recovery is so fast such that the effect of hardening is annihilated (hereinafter designated as the recovery).[3–5] Van Haaften *et al.*[3] experimentally showed the recovery behaviors of AA3104 and AA5182. Chobaut *et al.*[4] also revealed the plastic strain recovery behaviors for AA7449 and AA7040.

Constitutive equations of several types have been developed and used in previous studies for predicting the casting residual stress. In this paper, these equations are classified into elasto-plastic model, elasto-viscoplastic model, and elasto-plastic-creep model and are discussed on their capability of duplicating the above-mentioned metallurgical phenomena. Details of these equations were summarized in our earlier study.[2] This study discusses the general features of these equations for duplicating the recovery and strain-rate dependence. Although the classical elasto-plastic model has often been used in thermal stress analysis, especially for shape castings, Gustafsson *et al.*[6] and Motoyama *et al.*[7,8] predicted the residual stress of a stress lattice made of gray cast iron using the classical elasto-plastic model. Dong *et al.*[9] simulated the thermal stress of an aluminum casting with two cast-in stainless liners during casting and treated the aluminum casting as an elasto-plastic in the stress analysis. Hofer *et al.*[10,11] used the classical elasto-plastic model to predict the residual stress and distortion of high-pressure die castings. The classical elasto-plastic model cannot describe the strain-rate dependence because it includes no strain-rate terms. Furthermore, the model cannot consider recovery because the equivalent plastic strain developed at each temperature is included at the same degree in the hardening parameter. Our earlier work showed that excessive accumulation of the equivalent plastic strain engenders overestimation of the yield stress at low temperatures.[2] Consequently, the classical elasto-plastic model can be expected to overestimate the residual stress in castings. The strain-rate-dependent elasto-plastic model and elasto-viscoplastic model incorporate the strain-rate dependence. However, the models normally use the equivalent plastic strain or viscoplastic strain as the degree of strain-hardening; the models do not subtract a recovery strain component from the developed inelastic strain increment at high temperatures. Therefore, similar to the classical elasto-plastic model, the plastic or viscoplastic strain development at high temperatures causes unrealistic strain-hardening of the casting at low temperatures in strain-rate-dependent elasto-plastic and elasto-viscoplastic models. Alankar and Mary[5] used the extended Ludwik equation that is the commonly used elasto-viscoplastic model and showed that the simulation using its equation predicted the excess work hardening of AA5182 compared with the experiment at low temperatures during two-step deformation tests.

Several researchers have strived to incorporate recovery into the constitutive equation. van Haaften *et al.*[3] introduced a temperature-dependent hardening parameter into the Garofalo equation to duplicate the change of the recovery behavior from low to high temperatures. Thorborg *et al.*[12] proposed the usage of the temperature-dependent factor that showed the contribution ratio of the inelastic strain increment to the strain-hardening. Ejær and Mo[13] and Drezet *et al.*[14] used the "cut-off temperature" above which the strain-hardening was not taken into account. Alankar and Mary[5] divided the inelastic strain into a "creep" component where no plastic strain would be accumulated and a "plastic" component where plastic strain would be accumulated based on n-value of the extended Ludwik equation at each temperature. We also originally developed an elasto-plastic-creep constitutive equation that can represent the recovery behavior conveniently by introducing the creep term.[2] The strain-rate dependence can also be expressed in our equation. These constitutive equations have been evaluated by comparing the simulated thermal stress with the so-called "Continuous Cooling Test" (CCT).[5] In the test, an already solidified and machined tensile[3,5,15] or a casting specimen[16] cools with the thermal strain of the specimen being constrained using the experimental devices. The constraint of the thermal strain engenders thermal stress in the specimen during cooling. Continuous cooling tests present the benefit of allowing comparison not only of the final thermal stress but also of the thermal stress during cooling between the simulation and the experiment. However, previous studies have not produced a comprehensive understanding of how the recovery and strain-rate dependence influence the accuracy of predicting thermal stress during casting. Shiga *et al.*[16] revealed that using the elasto-plastic-creep constitutive equation considering the recovery and strain-rate dependence improved the accuracy of thermal stress prediction of Al-Si-Cu alloy during casting in the CCT. However, they did not separately investigate the effects of recovery and strain-rate dependence. Therefore, it remains unclear how and the extent to which each of the two factors affects the thermal stress prediction during casting in the study. Alankar and Wells[5] took the recovery into account in the modified Ludwik equation. They concluded that recovery should be considered in situations where the temperature is changing during the simulation. However, they did not also separate the effect of strain-rate dependence and recovery. van Haaften *et al.*[3] investigated the effects of considering the recovery, but their study has the same problem in the evaluation of constitutive equation. Individual evaluation of the strain-rate dependence and recovery was not discussed on the prediction accuracy of the CCT.

B. *Mechanical Properties for Thermal Stress Analysis of Al-Si-Cu Casting During Casting*

This type of casting aluminum alloy shows aging behavior even at RT: natural aging. Therefore, the tensile testing methodology affects the results of the obtained mechanical properties of the alloy. We have already revealed that the mechanical properties measured by the cooling test (C.T.) more closely approximated those during casting than the mechanical properties obtained by the conventional heating test (H.T.) did.[2] The C.T. is a tensile testing method by which the specimen is heated near the solidus temperature to dissolve the precipitate before cooling to a tensile testing temperature. Our earlier study showed that initial yield stresses obtained using conventional H.T. were 50–64 pct higher than those obtained using C.T. for Al-Si-Cu casting alloy. However, that earlier study did not reveal to what extent the different mechanical properties of the C.T. and H.T. affect the prediction accuracy of the thermal stress analysis during casting of Al-Si-Cu alloy.

This study was therefore undertaken to elucidate the effects of the following items on the prediction accuracy of the thermal stress of Al-Si-Cu alloy specimen during casting:

(1) choice of stress–strain curves of the Al-Si-Cu alloy obtained using C.T. or H.T.,
(2) recovery behavior, and
(3) strain-rate dependence.

First, this study compares the *in situ* thermal stress measured in the CCT with the analysis of elasto-plastic models using stress–strain curves obtained by H.T. and C.T. From the comparison, this study shows how important using curves of C.T. is for the accurate prediction of the thermal stress of the Al-Si-Cu alloy during casting. Second, to reveal each effect of considering (2) and (3) in the constitutive equation, this study used the classical elasto-plastic model, strain-rate-dependent elasto-plastic model, and our originally developed elasto-plastic-creep model.[2] The classical elasto-plastic model represented neither the strain-rate dependence nor the recovery. Although the strain-rate-dependent elasto-plastic model was able to represent the strain-rate dependence, the model did not represent the recovery. Our developed elasto-plastic-creep model represented both the strain-rate dependence and the recovery. The simulated thermal stresses obtained using each of the constitutive equations were compared with CCT measurement results. Finally, we provide guidelines for the constitutive equation of the Al-Si-Cu alloy in the prediction of the thermal stress during casting.

II. *IN SITU* THERMAL STRESS MEASUREMENT DURING CASTING

We include a brief mention about the CCT device developed already (Figure 1) and the CCT procedure used in this study.[16]

The device had an I-shaped cavity. Thermal contraction of its casting was constrained during cooling by the device. The developed longitudinal thermal stress due to the constraint was measured continuously using the load cell with decreasing temperature of the casting specimen. The device comprised metal molds for producing the flange of the casting and for constraining the thermal contraction of the casting, a framework composed of strut bars and rigid plates made of plain carbon steel, a load cell installed between the framework and the constraint metal molds, stainless screw parts and nuts for tightening the parts described above, stainless steel side molds for making the gage section of the I-shaped casting, and block-shaped insulators for making the upper and lower surface of the casting. The screw parts and nuts were tightened with a torque wrench to keep the tightening force constant during the experiments. Soft ceramic insulators were installed between the constraint molds and the side molds to prevent locking of the displacement of the constraint mold during cooling. The casting gage section length was 100 mm. The casting cross-section dimensions were 10 mm × 10 mm (Figure 2).

Before making the parts of the device, the dimensions of each part were determined from elastic stress analysis using FEM software so that the elastic deformation of the device was less than 10 pct compared to the amount of casting thermal contraction when the estimated

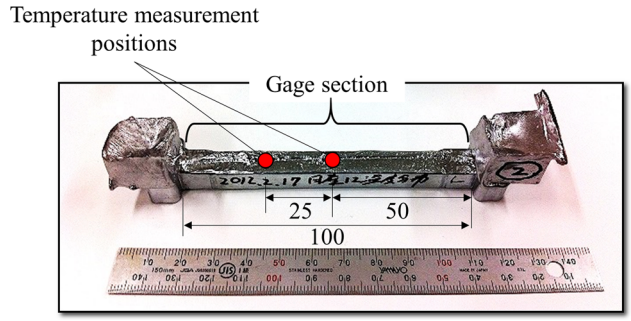

Fig. 2—Casting specimen of the CCT.

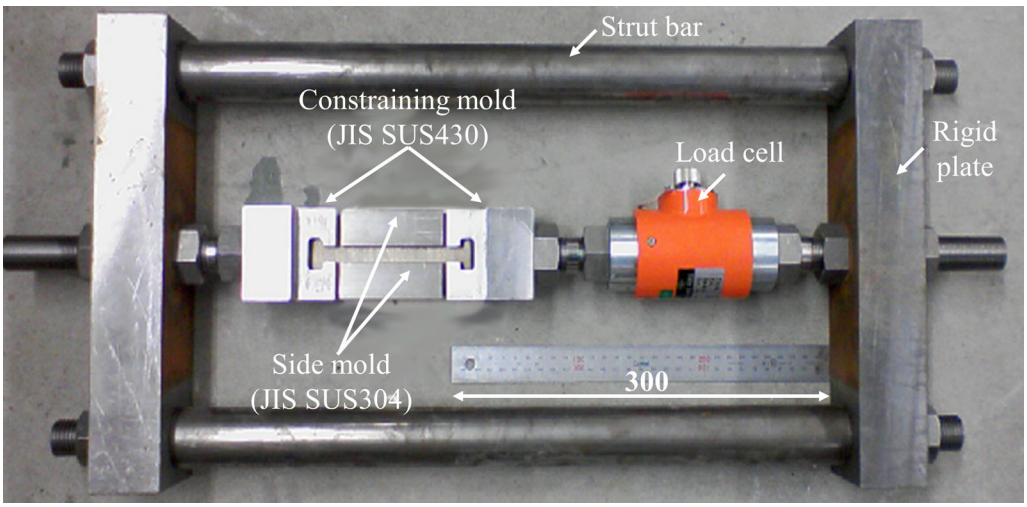

Fig. 1—Appearance of the developed continuous cooling test device Reprinted from Ref. [16].

Table I. Chemical Composition of AD12.1 Alloy for Casting

Si (Mass Pct)	Cu (Mass Pct)	Mg (Mass Pct)	Zn (Mass Pct)	Fe (Mass Pct)	Mn (Mass Pct)	Ti (Mass Pct)	Ni (Mass Pct)	Al (Mass Pct)
10.50	1.96	0.20	0.43	0.72	0.20	0.04	0.03	bal.

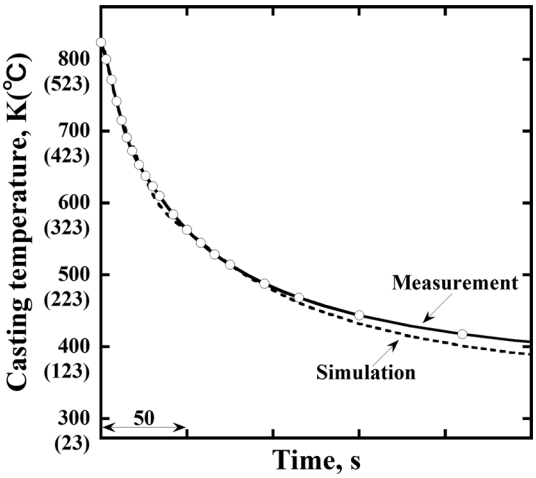

Fig. 3—Comparison of the simulated and measured casting temperatures at 25 mm from the center of the specimen during casting in the CCT (Reprinted from Ref. [16]).

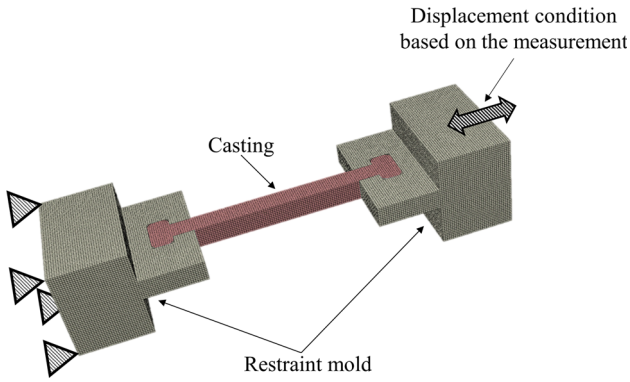

Fig. 4—Finite element model of the CCT (Reprinted from Ref. [16]).

maximum load was applied. The constraint mold displacement during the measurement was measured using linear variable differential transformers and was less than 10 pct compared with the casting thermal contraction in the actual experiments. Its data were used as the displacement condition of the constraint molds in the thermal stress analysis. The casting and mold temperatures were calculated using the type K ∅ 0.5-mm stainless sheathed thermocouples at the center of the casting and mold thickness. Temperature measurement positions of the casting are shown in Figure 2. A used Al-Si-Cu die casting alloy (Japanese Industrial Standard ADC12), the composition of which is presented in Table I, was melted at 1013 K (740 °C). The molten alloy was degassed by Ar gas blowing. The pouring temperature was 991 K (718 °C). The pouring time was approximately 1 s. The initial metal mold temperature was 298 K (25 °C). The experiment was

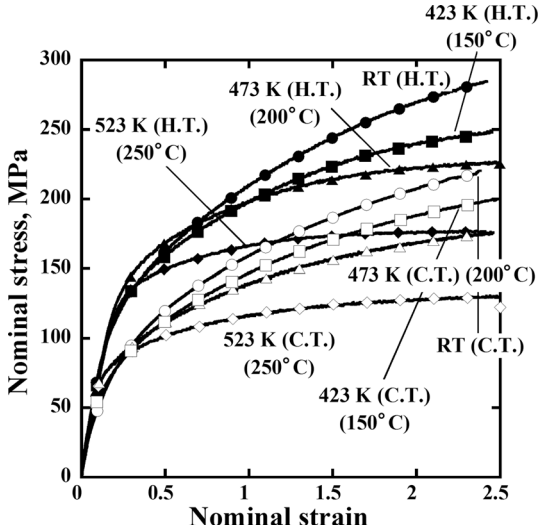

Fig. 5—Difference of stress–strain curves between H.T. and C.T.[2]

conducted twice, and the difference of the measured longitudinal thermal stress of the casting at 373 K (100 °C) was 2 pct in the two experiments. This means that high reproducibility was obtained in the experiments.

III. THERMAL ANALYSIS AND THERMAL STRESS ANALYSIS

A. *Thermal Analysis*

Thermal analysis was conducted using CapCast ver. 3.5.7 (EKK, Inc.). Thermal properties of the Al-Si-Cu aluminum alloy were obtained using JMatPro, which is a thermodynamic database (Sente Software Ltd.). The JMatPro results showed the respective alloy liquidus and solidus temperatures as 850 K (577 °C) and 764 K (490 °C). The other thermal properties of the alloy and metal molds are listed in the Appendix. When the inaccurate thermal analysis results of the casting are used as the temperature histories of the casting in the thermal stress analysis, the analysis cannot predict the thermal stress of the casting with high accuracy. In that case, it is difficult to discuss the prediction accuracy of the thermal stress analyses using the alloy constitutive equations including the recovery and/or the strain-rate dependence. Therefore, in this study, high reproducibility of the casting temperature was achieved by optimizing the heat transfer coefficient between the casting and the metal molds using a trial-and-error method. Figure 3 shows the comparison of the simulated and measured casting temperatures at 25 mm from the center of the specimen during cooling.[16] Errors in

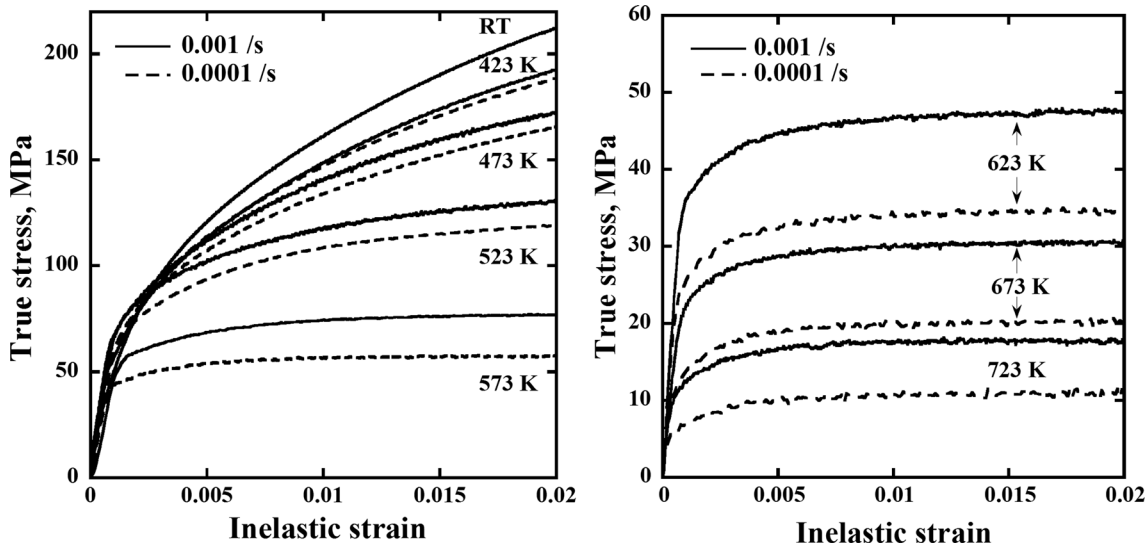

Fig. 6—Stress–inelastic strain curves of ADC12 measured by C.T. for the strain-rates 0.001 and 0.0001 /s from RT-723 K (RT-450 °C) (Reprinted from Ref. [16]).

Table II. Stress–Strain Curves of ADC12 Used for Determining Material Parameters of Each Constitutive Equation

	RT-423 K (RT-250 °C)	423 to 723 K (250 to 450 °C)	423 to 723 K (250 to 450 °C)
Elasto-Plastic model using H.T. data	stress–strain curves strained at 0.001 /s by H.T.	stress–strain curves strained at 0.001 /s by C.T.	estimated stress–strain curve from semi-solid tensile tests
Elasto-Plastic model using C.T. data	stress–strain curves strained at 0.001 /s by C.T.		estimated stress–strain curve from semi-solid tensile tests
Strain-dependent Elasto-Plastic model using C.T. data	stress–strain curves strained at 0.001 and 0.0001 /s by C.T.		estimated stress–strain curve from semi-solid tensile tests
Elasto-Plastic-Creep model using C.T. data	stress–strain curves strained at 0.001 and 0.0001 /s by C.T. (Only for 423 K (250 °C), averaged curve of 0.001 and 0.0001 /s was adopted)		estimated stress–strain curve from semi-solid tensile tests

temperature between the simulation and experiment were less than 25 K at all measuring points of the casting in thermal analysis. The measured casting temperature histories of the two points were almost the same. Therefore, in this study, the analyzed experimental results using the casting temperature at 25 mm from the center of the specimen are presented in Section IV.

B. *Thermal Stress Analysis*

Abaqus ver. 6.12-2 (Dassault Systemes) was used to conduct thermal stress analyses, which were done only for the casting and the constraint molds, as shown in Figure 4. The previously described thermal analysis results were used as the temperature history of the casting for thermal stress analysis.

C. *Constitutive Equations and Mechanical Properties of the Aluminum Casting*

1. *Constitutive equation used to investigate the recovery and strain-rate dependence*

For the elasto-plastic constitutive equation, this study used the following equations:[2]

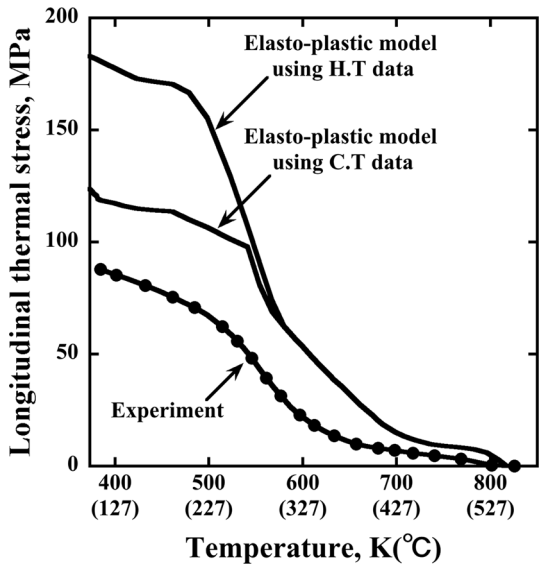

Fig. 7—Comparison of longitudinal stress of the casting among experiment, simulation using H.T. data, and simulation using C.T. data.

$$\varepsilon_{ij} = \varepsilon_{ij}^{e} + \varepsilon_{ij}^{p} \quad [1]$$

$$\sigma_{ij} = D_{ijkl}(T)\varepsilon_{kl}^{e} \quad [2]$$

$$f(\sigma_{ij}, T) = \sqrt{3J_2} - (\sigma_y(T) + K) \quad [3]$$

$$K = K(\varepsilon_{eff.}^{p}, T) \quad [4]$$

$$\dot{\varepsilon}_{ij}^{p} = \lambda \frac{\partial f}{\partial \sigma_{ij}}. \quad [5]$$

In those equations, T stands for the temperature, σ_{ij} denotes the stress, ε_{ij}^{e} signifies the elastic strain, ε_{ij}^{p} represents the plastic strain, D_{ijkl} is the elastic coefficient tensor, J_2 is the second invariant of the deviatoric stress tensor, and $\sigma_y(T)$ represents the initial yield stress, which is dependent on the temperature. In addition, $\varepsilon_{\text{eff}}^{p}$ stands for the equivalent plastic strain, λ denotes the positive scalar, and K is the hardening parameter, which is a function of temperature and equivalent plastic strain.

For the strain-rate-dependent elasto-plastic constitutive equation, this study used the following empirical equation. By changing $(\sigma_y(T) + K)$ in Eq. [3] to the following Eq. [6], the above-mentioned elasto-plastic model can take the strain-rate dependence of the stress–strain curve into account:[17]

$$\sigma_{ys} = \sigma_{ys}^{0}(\varepsilon_{eff.}^{p},\ T)R(\dot{\varepsilon}_{eff.}^{p},\ T). \quad [6]$$

Here, σ_{ys} is the yield stress, $\sigma_{ys}^{0}(\varepsilon_{eff.}^{p},\ T)$ is the yield stress obtained from a quasi-static tensile test at temperature T, and $R(\dot{\varepsilon}_{eff.}^{p},\ T)$ represents the ratio of yield stress obtained by stretching a specimen at strain-rate $\dot{\varepsilon}_{eff.}^{p}$ to that obtained by stretching at a quasi-static strain-rate. The same isotropic hardening rule and associated flow rule as the above-mentioned elasto-plastic model were adopted.

Our developed elasto-plastic-creep constitutive equation was used to evaluate the effects of considering the strain-rate dependence and recovery. The reproducibility of the stress–strain curves, that of strain-rate dependence, and recovery behavior of the equation were reported in detail in our previous study.[2]

2. *Mechanical properties of JIS ADC12 for the constitutive equations*

We have already obtained the stress–strain curves of the alloy by C.T. and H.T. (strain-rates: 0.001 and 0.0001 /s), as shown in Figures 5 and 6.[2]

These curves were used to determine the material properties of the constitutive equations. The elastic strain component was subtracted in the stress–strain curves at each temperature using Young's modulus of the alloy to obtain the stress–inelastic strain curves. Young's modulus at each temperature was measured by the resonance method.[2] The stress–strain curves of the alloy above solidus temperature were quoted from an earlier study in which tensile tests were conducted during alloy solidification.[18] The same coefficients of thermal expansion for the alloy as our earlier study were used and these values were obtained using JMatPro.[16]

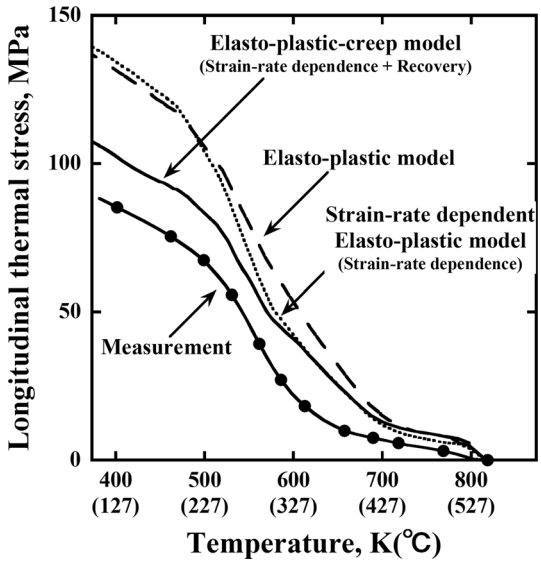

Fig. 8—Effect of recovery and strain-rate dependence in constitutive equation on prediction accuracy of thermal stress analysis during casting.

Table III. Effect of the Kind of Constitutive Equation on the Prediction Accuracy of Longitudinal Thermal Stress of Casting at 373 K (100 °C)

	Longitudinal thermal stress of casting at 373 K (MPa)	Ratio*
Measurement	90.2	
Elasto-Plastic model using H.T. data	182.8	2.03
Elasto-Plastic model using C.T. data	135.4	1.50
Strain-dependent Elasto-Plastic model using C.T. data (model including strain-rate dependence)	138.1	1.53
Elasto-Plastic-Creep model using C.T. data (model including strain-rate dependence + recovery)	106.4	1.18

*Ratio of simulated value to experimental value.

(1) Assessment of stress–strain curves of C.T. and H.T. for thermal stress analysis during casting

The simulation results obtained using the stress–strain curves of C.T. were compared with the results obtained using those of the conventional H.T. in the elasto-plastic model. Stress–strain curves of C.T. were used at temperatures higher than 573 K (300 °C) in the elasto-plastic model using H.T. curves because the available stress–strain curves of H.T. were only from RT to 523 K (RT to 250 °C). The stress–strain curves of C.T. and H.T. obtained at the strain-rate of 0.001 /s were used for the elasto-plastic model.

(2) Effects of considering recovery and strain-rate dependence

Only the stress–strain curves of C.T. were used for the elasto-plastic model, strain-rate-dependent elasto-plastic model, and elasto-plastic-creep model. In the elasto-plastic constitutive equation, data of stress–inelastic strain relations were inputted in tabular form for each temperature. Therefore, the elasto-plastic model can accurately reproduce the strain-hardening transient of the stress–inelastic strain curves. In the strain-rate-dependent elasto-plastic constitutive equation, the stress–inelastic strain curve of 0.0001/s strain-rate was inputted for $\sigma_{ys}^{0}(\bar{\varepsilon}_{eff.}^{p},\ T)$ in tabular form for each temperature. Therefore, the strain-rate-dependent elasto-plastic model also duplicates the strain-hardening behavior of each temperature. $R(\dot{\bar{\varepsilon}}_{eff.}^{p},\ T)$ values were determined by calculating the ratios of the yield

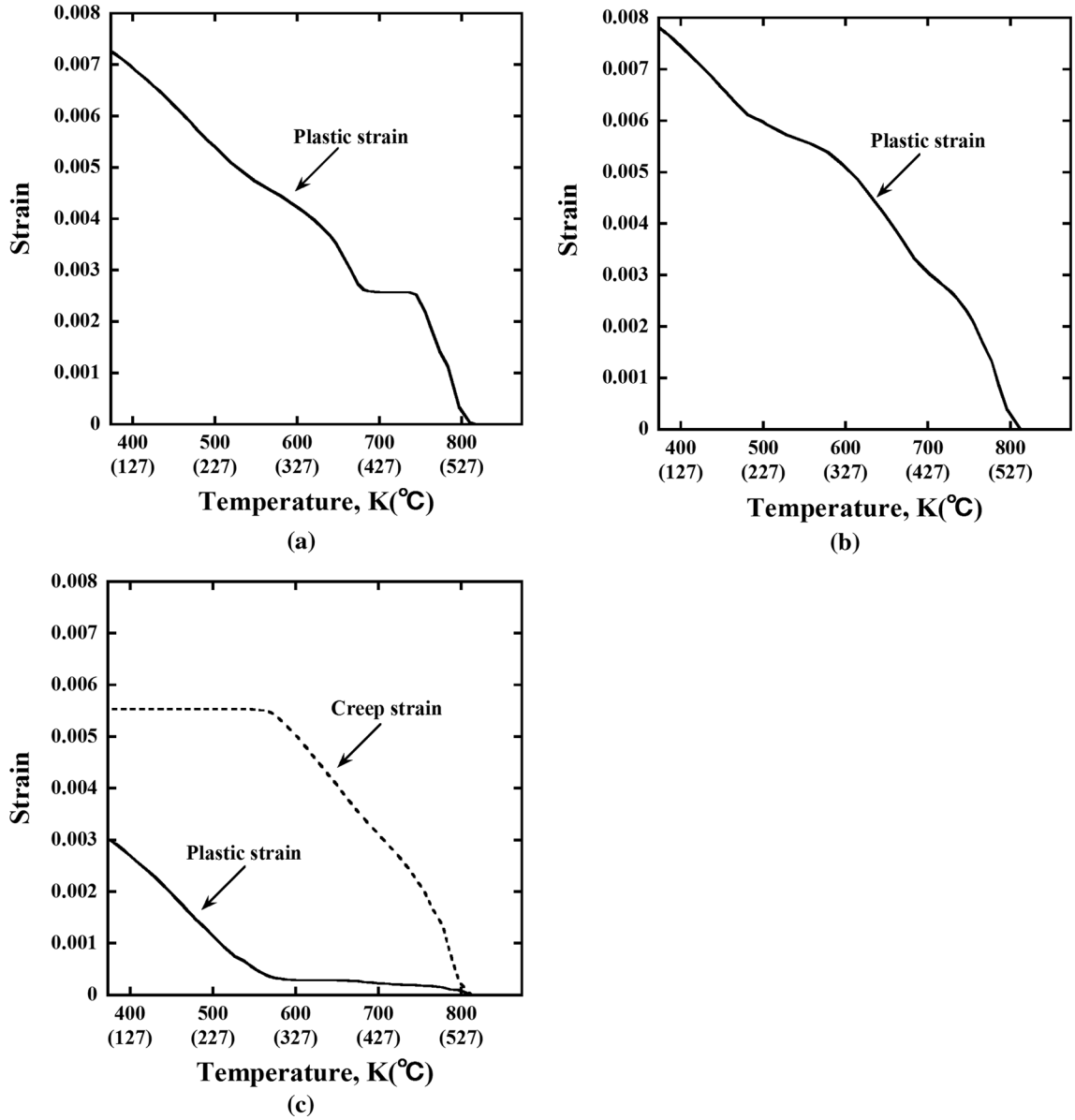

Fig. 9—Development of longitudinal inelastic strains in the gage section of the casting during cooling: (*a*) Elasto-Plastic model, (*b*) Strain-rate-dependent Elasto-Plastic model, and (*c*) Elasto-Plastic-Creep model.

stress of strain-rate 0.0001 /s to those of 0.001 /s at each temperature. The material parameters of the elasto-plastic-creep constitutive equation were the same as those of our previous study.[2] The used material parameters and the reproduction accuracy of the strain-hardening transient of JIS ADC12 were described in detail in the study. Table II presents the stress–strain curves used for determining the material constants of the constitutive models described above.

IV. RESULTS AND DISCUSSION

A. *Effect of Choosing C.T. and H.T. on the Simulated Thermal Stress During Casting*

Figure 7 presents the effects of the stress–strain curves of C.T. and H.T. on the simulated thermal stress during casting in the elasto-plastic model.

Both models overestimate the thermal stress during casting. At temperatures higher than 573 K (300 °C), the simulated thermal stress is the same between the two models because the same C.T. curves were inputted for both models at temperatures higher than 573 K (300 °C), as described in Section III–C–2 1. Below approximately 573 K (300 °C), the model using H.T. curves gradually shows higher thermal stress of the casting than that of the model using C.T. curves. Finally, the simulated thermal stress of the model using H.T. curves becomes 35 pct higher than that of the model using C.T. curves at 373 K (100 °C), giving results that are 203 pct higher than those obtained from the experiment, as shown in Table III because yield stresses of H.T. were increased by natural aging and its precipitate state differed from that during casting.[2] Therefore, thermal stress analysis during casting for the precipitation hardening-type aluminum casting should use the stress–strain curves obtained by C.T. where the precipitate of the tensile specimen dissolves by the solution heat treatment. However, there is still 50 pct error in the elasto-plastic model using C.T. data, as shown in Table III.

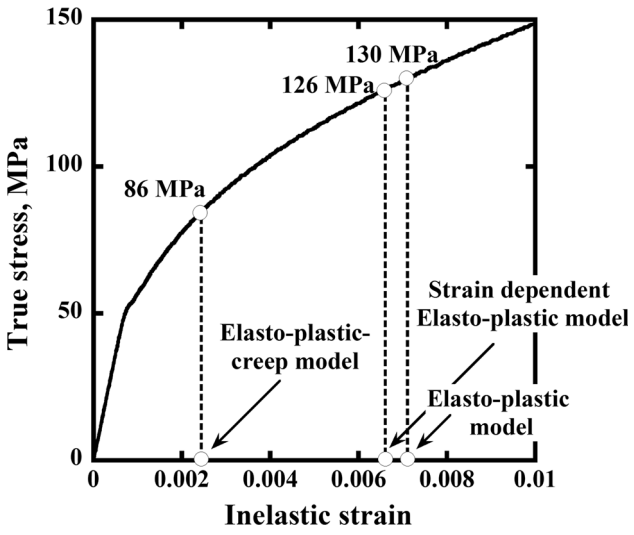

Fig. 10—Effective plastic strain of each model accumulated in the gage section of the casting until 423 K (150 °C) and stress–inelastic strain curve of ADC12 obtained at 423 K (150 °C) by C.T.

B. *Effects of Recovery and Strain-Rate Dependence on Prediction Accuracy of Thermal Stress Analysis During Casting*

Figure 8 presents the thermal stress of casting in its longitudinal direction between the measurement and calculation results simulated by the elasto-plastic, strain-rate-dependent elasto-plastic, and elasto-plastic-creep constitutive equations using stress–strain curves of C.T.

In the elasto-plastic model, the simulated thermal stress was overestimated compared with the experiment from the end of solidification to 373 K (100 °C). In addition, the thermal stress prediction accuracy was poorer than the other two constitutive equations in all temperature ranges. As described below in greater detail, the excessive simulated thermal stress at low temperatures is explained by the lack of consideration of the recovery. That lack induced the accumulation of effective inelastic strain at high temperatures and caused an unrealistic increase in the yield stress at low temperatures. At high temperatures, comparison of results with those of the other models shows that the error was a lack of incorporating the strain-rate dependence, as described below.

In the strain-rate-dependent elasto-plastic constitutive equation, the accuracy of thermal stress prediction was better than that of the elasto-plastic model from the end of the solidification to approximately 623 K (350 °C). The Al-Si-Cu alloy shows strong strain-rate dependence in this temperature range, as shown in Figure 6. Therefore, compared with the elasto-plastic model, the accuracy of thermal stress prediction in the high temperature range was improved by the strain-rate-dependent elasto-plastic model, which was able to consider the strain-rate dependence. The elasto-plastic-creep model also incorporated the strain-rate dependence. The prediction accuracy of thermal stress improved from the end of the solidification to approximately 623 K (350 °C) as with the strain-rate-dependent elasto-plastic model. However, the error between the simulated and measured values increased gradually at temperatures less than 623 K (350 °C) in the strain-rate-dependent elasto-plastic model. Eventually, for the strain-rate-dependent elasto-plastic model, no improvement was observed in the final thermal stress versus the elasto-plastic model. The strain-rate-dependent elasto-plastic model did not incorporate recovery. Therefore, excess thermal stress developed at low temperatures for the same reason as occurred in the elasto-plastic model.

Among the three models used in this study, the elasto-plastic-creep model predicted the thermal stress of the casting most accurately, not only at high temperatures but also at low temperatures. In the elasto-plastic-creep model, recovery prevents the effective inelastic strain on strain-hardening at high temperatures from accumulating: excess yield stress at low

temperatures was avoided. At high temperatures, consideration of the strain-rate dependence contributed to improvement of the prediction accuracy.

To elucidate details of the effects of recovery, the inelastic strains developed at the gage section of the casting in the longitudinal direction of the casting such as the plastic and creep were investigated in the three constitutive equations, as shown in Figure 9.

Figures 9(a) and (b), respectively, present the results of the elasto-plastic and strain-rate-dependent elasto-plastic models. Both plastic strains developed continuously from the end of solidification. These figures clearly show that strain-hardening also progressed continuously with the development of plastic strain in the two models. Figure 10 shows the effective plastic strain amount of the gage section on strain-hardening in each model that accumulated until 423 K (150 °C) and the stress–inelastic strain curve of ADC12 obtained at 423 K (150 °C) by C.T. This graph presents the degree of strain-hardening in the gage section of the casting at 423 K (150 °C) in each constitutive equation. In the elasto-plastic model, the plastic strain reached 0.0071 at 423 K (150 °C). This result indicates that the yield stress reached 130 MPa at the gage section of the casting at 423 K (150 °C). In the strain-rate-dependent elasto-plastic model, the plastic strain reached 0.0066 at 423 K (150 °C). At that temperature, the yield stress at the gage section of the casting reached 126 MPa. However, in the elasto-plastic-creep model at temperatures higher than 573 K (300 °C), almost all of the inelastic strain developed not as the plastic strain but as the creep strain at temperatures higher than 573 K (300 °C), as shown in Figure 9(c). Below 573 K (300 °C), development of the creep strain stopped, and the inelastic strain alternatively developed as the plastic strain. When the casting temperature was 423 K (150 °C), the plastic strain reached 0.0024. The yield stress was 86 MPa in the gage section of the casting, as shown in Figure 10, which indicates that the strain-hardening did not progress compared with the other models. Therefore, the quasi-incorporation of the recovery using the creep strain term in our developed elasto-plastic-creep model prevented the plastic strain that contributed to strain-hardening from accumulating at high temperatures. As a result, the incorporation of the recovery contributed to the improvement of the thermal stress at low temperatures. Table III presents the accuracy of thermal stress prediction in the longitudinal direction of the casting at 373 K (100 °C) in each model.

Based on the discussion presented above, this study obtained the following guidelines for the constitutive equation used in the thermal stress analysis of precipitation hardening-type aluminum casting during casting.

The strain-rate dependence should be incorporated into the constitutive equation to predict defects accurately where the thermal stress developed at a high temperature is crucially important. For example, a hot tear is a typical defect in this case. The recovery should be considered in the constitutive equation for accurate prediction of defects such as residual stress, warpage, and cold cracking. These defects require accurate prediction of the thermal stress developed at low temperature. Therefore, an unrealistic increase of yield stress at low temperatures should be avoided by incorporating the recovery behavior in the constitutive equation.

V. CONCLUSIONS

Thermal stress analysis of an I-shaped Al-Si-Cu casting was conducted. Then the results were compared with the *in situ* measured values. This comparison revealed the following guidelines related to the constitutive equation of the precipitation hardening-type aluminum casting alloy for thermal stress analysis during casting.

(1) Stress–strain curves obtained by conventional H.T. method should not be used to determine the constitutive equation parameters of precipitation hardening-type aluminum alloy during casting. The elasto-plastic model using H.T. data estimated more than twice the final thermal stress of the I-shaped casting compared with the measured value.
(2) The constitutive equation parameters of precipitation hardening-type aluminum alloy during casting should be determined based on the stress–strain curves of C.T., with the aim of dissolving the precipitate in the tensile specimen. The accuracy of thermal stress prediction using H.T. curves described above was improved drastically using the stress–strain curves of C.T.
(3) The Al-Si-Cu die casting alloy (JIS ADC12) used in this study showed strong strain-rate dependence at temperatures higher than 623 K (350 °C). The prediction accuracy of thermal stress developed in this temperature range was improved by the incorporation of strain-rate dependence into the constitutive equation of the alloy.
(4) With a constitutive equation that incorporated the recovery, the prediction accuracy improved in the thermal stress developed at low temperatures in the Al-Si-Cu alloy casting.
(5) Our originally developed elasto-plastic-creep model can describe both the strain-rate dependence and the recovery. Our equation predicted the thermal stress of the casting developed from high to low temperatures more accurately than the other elasto-plastic model and strain-rate-dependent elasto-plastic model.

APPENDIX: THERMAL PROPERTIES OF JIS ADC12 AND METAL MOLDS FOR THE THERMAL ANALYSIS

Figure A1 shows the thermal properties of JIS ADC12 for the thermal analysis of CCT. For the

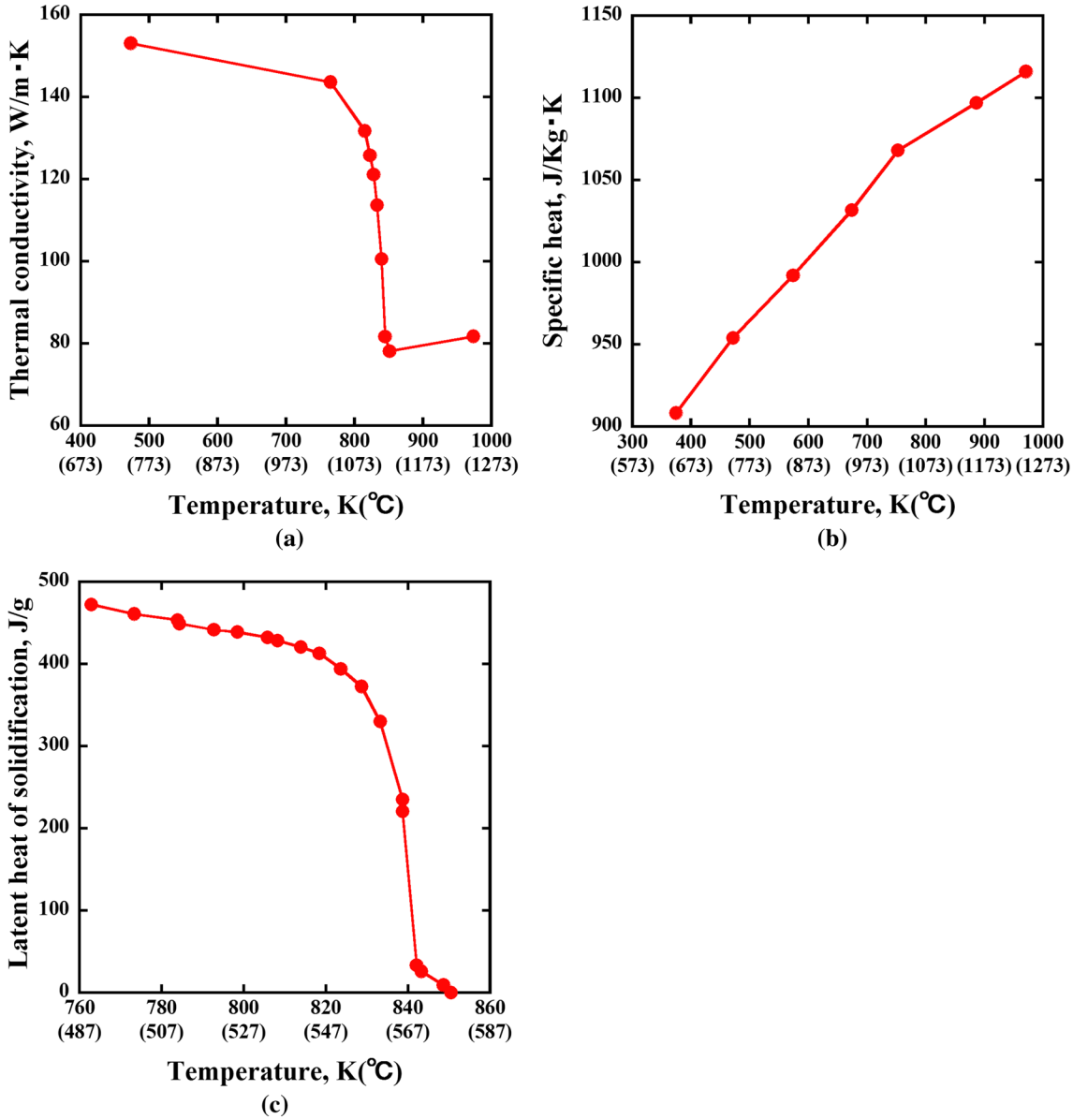

Fig. A1—Thermal properties of JIS ADC12 for thermal analysis: (*a*) thermal conductivity, (*b*) specific heat, and (*c*) release of latent heat of solidification with casting temperature.

density, temperature-independent values were used for the liquid and solid states, respectively. The density of liquid state was 2540 kg/m3, and that of solid state was 2610 kg/m3.

Figure A2 shows the thermal properties of stainless metal molds used for the thermal analysis. These molds are shown in Figure 1. The density of JIS SUS304 was 7930 kg/m3 and that of JIS SUS430 was 7700 kg/m3.

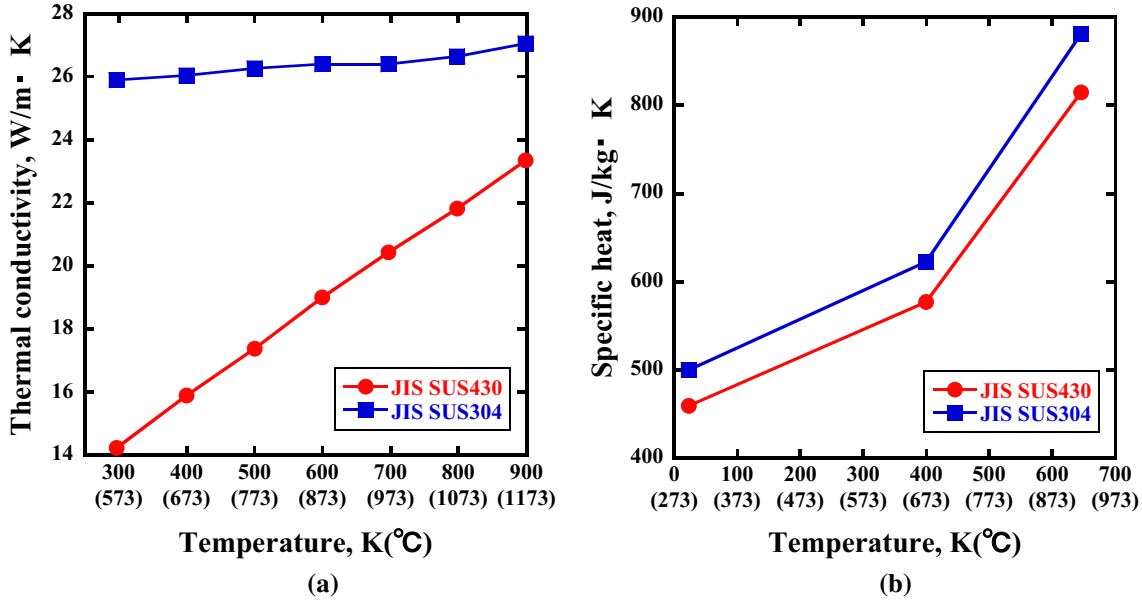

Fig. A2—Thermal properties of the metal molds for thermal analysis: (*a*) thermal conductivity and (*b*) specific heat.

REFERENCES

1. M.J. Roy, D.M. Maijer, and L. Dancoine: *Mater. Sci. Eng. A*, 2012, vol. 548, pp. 195–205.
2. Y. Motoyama, H. Shiga, T. Sato, H. Kambe, and M. Yoshida: *Metall. Mater. Trans. A*, 2016, vol. 47, pp. 5598–5608.
3. W.M. van Haaften, B. Magnin, W.H. Kool, and L. Katgerman: *Metall. Mater. Trans. A*, 2002, vol. 33, pp. 1971–80.
4. N. Chobaut, D. Carron, S. Arsène, P. Schloth, and J.-M. Drezet: *J. Mater. Process. Technol.*, 2015, vol. 222, pp. 373–80.
5. A. Alankar, M.A. Wells: Mater. Sci. Eng. A, 2010, vol. 527, pp. 7812–20.
6. E. Gustafsson, M. Hofwing, and N. Strömberg: *J. Mater. Process. Technol*, 2009, vol. 209, pp. 4320–28.
7. Y. Motoyama, H. Takahashi, T. Okane, Y. Fukuda, and M. Yoshida: *Metall. Mater. Trans. A*, 2013, vol. 44, pp. 3261–70.
8. Y. Motoyama, D. Inukai, T. Okane, and M. Yoshida: *Metall. Mater. Trans. A*, 2014, vol. 45, pp. 2315–25.
9. S. Dong, Y. Iwata, Y. Sugiyama, and H. Iwahori: *Mater. Trans.*, 2010, vol. 51 (2), pp. 371–76.
10. P. Hofer, E. Kaschnitz, and P. Schumacher: *Mater. Sci. Eng.*, 2012, vol. 33, p. 012055.
11. P. Hofer, E. Kaschnitz, and P. Schumacher: *JOM*, 2014, vol. 66, pp. 1638–46.
12. J. Thorborg, J. Klinkhammer, and M. Heitzer: *Mater. Sci. Eng.*, 2015, vol. 84, p. 012037.
13. H.G. Ejær and A. Mo: *Metall. Mater. Trans. B*, 1990, vol. 21, pp. 1049–61.
14. J.-M. Drezet, O. Ludwig, C. Jacquerod, and E. Waz: *Int. J. Cast Metals Res.*, 2007, vol. 20, pp. 163–70.
15. I. Farup and A. Mo: J. Therm. Stress., 2000, vol. 23, pp. 47–58.
16. H. Shiga, T. Sato, H. Kambe, Y. Motoyama, and Y. Makoto: *J. Jpn. Foundry Eng. Soc.*, 2015, vol. 87, pp. 453–59.
17. Abaqus 6.10-2 Analysis User's Manual. Dassault Systèmes Simulia Corp., Providence, vol. 3, p. 251.
18. K. Shinji, H. Takahashi, Y. Motoyama, and M. Yoshida: *J. Jpn. Inst. Light Metals*, 2013, vol. 63, pp. 253–59.